Hindawi Publishing Corporation
Journal of Biomedicine and Biotechnology
Volume 2010, Article ID 572570, 10 pages
doi:10.1155/2010/572570

Research Article

Preparative Separation and Enrichment of Syringopicroside from *Folium syringae* Leaves with Macroporous Resins

Xin Liu,[1] Jianming Wang,[2] Changxin Zhou,[1] and Lishe Gan[1]

[1] *College of Pharmaceutical Sciences, Zhejiang University, Hangzhou 310058, China*
[2] *Academy of Traditional Chinese Medicine, Heilongjiang University of Chinese Medicine, Harbin 150040, China*

Correspondence should be addressed to Xin Liu, xinliu98@126.com

Received 14 April 2010; Accepted 28 November 2010

Academic Editor: Yong Lim

Syringopicroside is the major constituent in *Folium syringae* leaves with known pharmacological activities. In this study, a simple method for preparative separation of syringopicroside from *F. syringae* leaves with macroporous resins was developed. Adsorption characteristics of syringopicroside on six types of macroporous resins, including ADS-8, ADS-17, D141, NKA-9, HPD450, and HPD600, have been compared, among which D141 resin showed the best adsorption and desorption capacities for syringopicroside. Adsorption isotherms were used to D141 resin at different temperatures and fitted well to Langmuir and Freundlich equations. Dynamic adsorption and desorption tests were performed on D141 resin-packed column to optimize the separation process of syringopicroside. After one run with D141 resin, the content of syringopicroside was increased 24-fold from 2.32% to 55.74% with a recovery yield of 92.16%. The chromatographic process optimized in this work avoids toxic organic solvent and, thus, is a promising basis for large-scale preparation of syringopicroside.

1. Introduction

Folium syringae is one of the popular ornamental and horticultural bushes cultivated in the middle latitudes of Eurasia and North America. This plant can cleanse air and be used as an indicator of the state of sulphur pollution [1]. Its leaves have been used extensively as one of the traditional Chinese folk herbs to treat various diseases, such as chordapsus, bacillary dysentery, icteric hepatitis, upper respiratory tract infection, and acute mastitis [2]. Two preparations of *F. syringae* such as Yanlixiao capsules and tablets, have been listed in Drug Standard of Ministry of Public Health of China [3]. Phytochemical investigations showed that syringopicroside (Figure 1), an iridoid glycoside, is the major active constituent in *F. syringae* leaves and possesses significant anti-inflammatory, broad-spectrum antimicrobial, antiviral [4, 5], and immune enhancement effects [6]. Therefore, the enrichment and separation of syringopicroside is indispensable for indepth pharmacological research and medical practice.

Up to now, several methods for the separation of syringopicroside have been reported. The reported methods, however, had some drawbacks. Syringopicroside was obtained conventionally by extracted with polar solvents including water, ethanol, and methanol through room temperature extraction, decoction and alcohol precipitation, sonication extraction, and refluxing extraction, then followed by multistep partition between different solvents such as diethyl ether, chloroform, and ethyl acetate [7–9], which led to poor purity and lower yields. Although this compound could be obtained by repeated preparative column chromatography using silica gel, C_{18} reveresed phase, and Sephadex LH-20 as chromatography media, these methods are time consuming and laborious, solvent wastage with extremely lower recovery, and thus they have limited industrial use [9–14]. Alternatively, macroporous resins have been successfully used in the separation and enrichment of bioactive compounds from plant materials owning to its simple procedure and high efficiency [15–17]. The ideal pore structure and various surface functional groups enabled highly selective adsorption capacity; meanwhile, they are

durable polar, nonpolar, or slightly hydrophilic polymers with relative low cost, easy regeneration and satisfied recovery of the adsorbed molecules [18, 19]. Macroporous resin column chromatography uses ethanol-water system as elution solvent, which is green and environment friendly. There is an increasing interest in employing macroporous resins to separate bioactive compounds in industrial practices [20, 21].

In the previous study, the authors separated syringopicroside from remainder extracts by using AB-8 macroporous resin [22]. However, thermodynamic properties of adsorption on macroporous resin and detailed technical conditions were not illustrated in the report. Furthermore, the content of syringopicroside in the final products was less than 50%, and the efficiency of separation was unsatisfied under the former type of resin column chromatography. Therefore, the present study was carried out to investigate the adsorption and desorption properties of syringopicroside on various macroporous resins with different polarities, aiming to develop an efficient method for the enrichment and preparative separation of syringopicroside with the optimal resin. The thermodynamic equilibrium properties for adsorption of syringopicroside on the selected resin were evaluated and analyzed the adsorption isotherms using empirical equations. The detailed technical conditions studies were further made for the adsorption and desorption of syringopicroside on D141 resin column chromatography. The results in this study provide a method for the large-scale enrichment and purification of syringopicroside from the extracts of *F. syringae* leaves.

2. Experimental

2.1. Sample, Chemicals, and Reagents. *F. syringae* leaves were collected in autumn 2008, in Heilongjiang Province, China. The botanical origin of material was identified by Professor Jianming Wang, and the voucher specimens were deposited at Institute of Traditional Chinese Medicine, Heilongjiang University, China.

Standard syringopicroside was prepared in our lab using repeated normal and reversed-phase column chromatography. Its structure was identified by comparison of the spectral data (ESIs-MS, ^{1}H NMR, and ^{13}C NMR) with those reported in the literature [23]. The purity of syringopicroside was determined to be more than 98% by normalization of the peak areas detected by HPLC-UV. The structure is shown in Figure 1.

Methanol (HPLC grade) was purchased from Merck (Darmstadt, Germany). All the other reagents were of analytical grade and purchased from Beijing Chemicals Industrial Reagents Ltd. (Beijing, China). Deionized water was purified by a Milli-Q water-purification system named Millipore (Bedford, MA, USA).

2.2. Adsorbents. Macroporous resins including ADS-8, ADS-17, NKA-9 HPD450, HPD600, and D141 were provided by Chemical plant of Nankai University (Tianjin, China), Cangzhou Bon Co., Ltd. (Hebei, China), and Chenguang

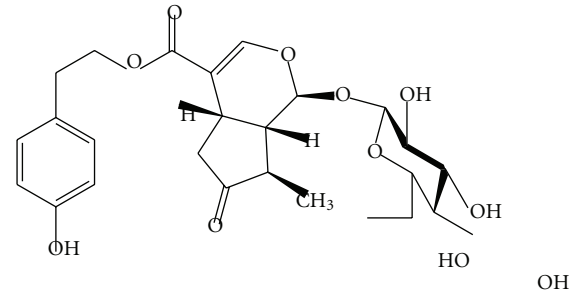

Figure 1: The chemical structure of syringopicroside.

Research Institute of Chemical Industry (Chengdu, China), respectively. The physical properties of these resins are summarized in Table 1. Prior to use, the resins were pretreated by soaking in 95% ethanol for 24 h and then eluting under reflux until there was no residue after distillation to remove the monomers and porogenic agents trapped inside the pores during the synthesis process. The resins were finally washed with deionized water until the ethanol was thoroughly replaced before use [24].

2.3. Determination of Moisture Content of Resins. Six tested macroporous resins were weighed, then placed in a drying oven, and dried at 70°C to constant weight [25]. The moisture contents of different resins are summarized in Table 1.

2.4. Preparation of F. syringae Leaves Extracts Sample Solutions. The leaves of *F. syringae* were ground into powders and then sieved (14 mesh). This powder (500 g) was extracted by refluxing with 6000 mL of deionized water for 2 h, and this was repeated two times. The extracted solutions were combined, filtered, and then concentrated to 1500 mL by a rotary evaporator under reduced pressure. The concentrates were precipitated by adding ethanol to a ratio of ethanol-water 70 : 30 (v/v), followed by centrifuging at 6000 rpm for 15 min. The supernatant extracts were concentrated at 50°C under vacuum to one-twentieth of the original volume by removing the ethanol solvent, which contained 2.32% syringopicroside. Deionized water was added to make a sample solution at the concentration of syringopicroside 4.92 mg/mL.

2.5. HPLC Analysis of Syringopicroside. HPLC analysis of syringopicroside was carried out on Waters 2695 liquid chromatographic system (Waters corp., USA) composed of Millennium system software, Model Waters Delta 600 quaternary pump with a degasser, a thermostat column compartment, and Model Waters 2998 Photodiode Array Detector (PAD). Chromatographic separation was performed on a Diamonsil (TM) C18 reversed-phase column (250 mm × 4.6 mm, 5 μm, USA) fitted with an Alltech C18 guard cartridge (8 mm × 4.6 mm I.D., 5 μm). The mobile phase was methanol-water-orthophosphoric acid (40 : 59.8 : 0.2, v/v/v). The injection volume was 10 μl

and flow rate was 1 mL/min. The column temperature was maintained at 25°C. Syringopicroside in the effluent was monitored at 221 nm by PAD detector, and the retention time was 22.36 min. The chromatographic peak of syringopicroside was confirmed by comparing its retention time and UV spectrum with that of the reference compound. The working calibration curve of syringopicroside showed good linearity over the range of 0.17–1.39 μg. The regression line for syringopicroside was $Y = 2.79 \times 10^6 X = 8.23 \times 10^4$ ($r = 0.9999$), where Y is the peak area and X is the quantity of syringopicroside (μg).

2.6. Static Adsorption and Desorption Tests. The static adsorption and desorption tests of *F. syringae* leaves extracts on macroporous resins were performed as follows: preweighed amounts of different hydrated test resins (equal to 5 g dry resin) were put into an Erlenmeyer flask with a lid, and 40 mL of sample solution (4.92 mg/mL syringopicroside) was added. The flasks were sealed tightly and shaken on an incubation shaker (100 rpm) at 25°C for 12 h to reach adsorption equilibrium. The solution after adsorption was gained by filtration and subjected to further HPLC analysis. Subsequently, the resin was washed with deionized water for 3 times and then desorbed with 80 mL ethanol-water (80 : 20, v/v) solution. The content of syringopicroside in solution after desorption was analyzed by HPLC in the same way. The candidate resins were screened in terms of their adsorption capacities, desorption capacities, and desorption ratios.

The adsorption isotherm of syringopicroside extracts on the selected resins was investigated by contacting 50 mL of sample solutions at various initial concentrations with preweighed amount of hydrated resins (equal to 5 g dry resin) on an incubation shaker (100 rpm) at 25°C, 30°C, and 35°C for 12 h, respectively. The concentrations after adsorption at different temperatures were monitored by HPLC at certain time intervals till equilibrium, and their degrees of fitness to Freundlich and Langmuir equations were evaluated.

The adsorption and desorption properties of preliminary chosen resin under different conditions including sample solution pH value and ion concentration were also compared.

2.7. Dynamic Adsorption and Desorption Tests. Dynamic adsorption and desorption experiments were carried out on glass columns (1.5 cm × 30 cm) wet-packed with the pretreated hydrated selected resin (equal to 15 g dry resin). The bed volume (BV) of the resin was 30 mL. In adsorption process, the effects of the ratio of column height to diameter and feeding flow rate on adsorption were optimized. While reaching adsorption equilibrium, the loading of the sample was stopped. The adsorbate-laden column was washed firstly by 4 BV deionized water and then eluted with different concentrations of ethanol-water solutions (30 : 70, 50 : 50, 70 : 30, 90 : 10, v/v) at a flow rate of 1 BV/h to select the optimal elution solution. The proper desorption flow rate of the optimal elution solution was evaluated by comparing the elution flow rate of 1, 2, 3, 4, and 5 BV/h, respectively. The eluted aliquots collected at 5 mL intervals by an autofractional collector, and the concentration of syringopicroside in each part of desorption solution was determined by HPLC.

2.8. Recovery of Syringopicroside with D141 Resin Column Chromatography. Recovery was determined by calculating the content of syringopicroside in the extracts before and after purification on column packed with D141 resin to evaluate the accuracy of the method. The equation of recovery was described by the following mathematical formula:

$$R(\%) = \frac{\text{the content of syringopicroside after column}}{\text{the content of syringopicroside before column}} \times 100\%. \quad (1)$$

3. Results and Discussion

3.1. Adsorption and Desorption Capacities—Desorption Ratio. The following equations were applied to quantify the capacities of adsorption and desorption as well as the ratio of desorption.

Adsorption evaluation

$$q_e = \frac{(C_0 - C_e)V_i}{(1 - M)W}, \qquad E(\%) = \frac{(C_0 - C_e)}{C_0} \times 100\%, \quad (2)$$

where q_e denotes the adsorption capacity at adsorption equilibrium (mg/g dry resin); E is the adsorption ratio, which means percentage of total adsorbate at adsorption equilibrium; C_0 and C_e are the initial and equilibrium concentrations of solutes in the solutions, respectively (mg/mL); V_i is the volume of the initial sample solution (mL); M represents the ratio of water content; W is the weight of the test resins (g).

Desorption evaluation

$$q_d = \frac{C_d V_d}{(1 - M)W}, \qquad D(\%) = \frac{C_d V_d}{(C_0 - C_e)V_i} \times 100\%, \quad (3)$$

where q_d is the desorption capacity after adsorption equilibrium (mg/g dry resin); C_d is the concentration of solutes in the desorption solution (mg/mL); V_d is the volume of the desorption solution (mL); D is the desorption ratio (%); C_0, C_e, V_i, and M are the same as described above.

Six macroporous resins with different physical properties were screened for the adsorption and desorption tests, and the results were listed in Figure 2. The adsorption and desorption capacities of the resins correlated with the properties of the resins and the chemical features of the adsorbed substance. As shown in Figure 2, NKA-9 resin shows poor adsorption capacity owing to its relatively lower surface area. The considerably higher adsorption capacities and lower desorption ratios of HPD450 and HPD600 resins towards

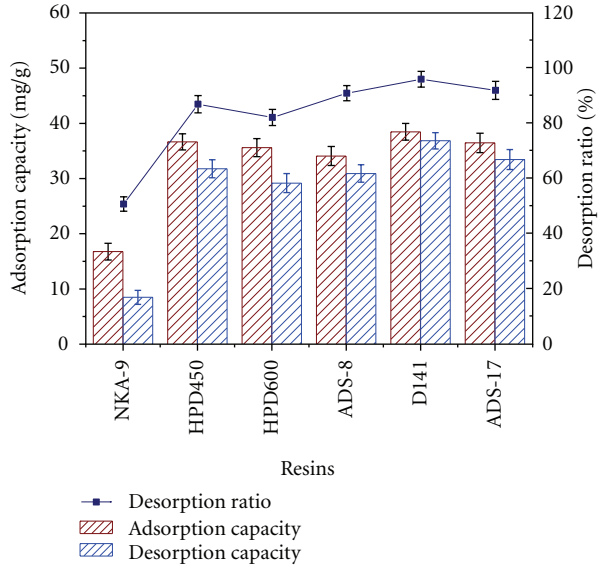

Figure 2: Adsorption and desorption capacities and desorption ratio of syringopicroside on different resins ($n = 3$). Data are expressed as the mean ± standard deviation (Mean ± SD).

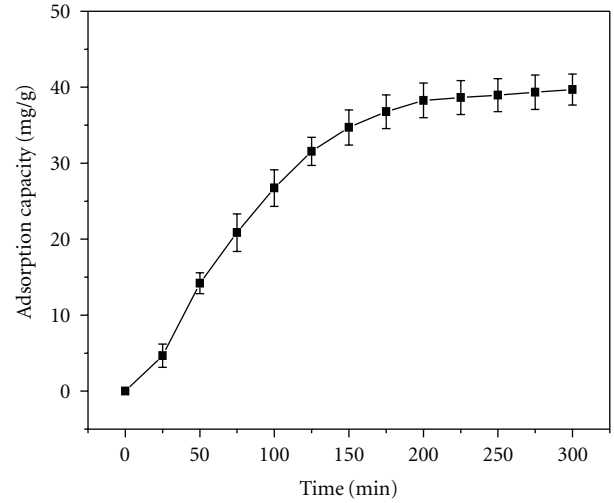

Figure 3: Adsorption kinetics curve for syringopicroside on D141 resin ($n = 3$). Data are expressed as the mean ± standard deviation (Mean ± SD).

syringopicroside could be explained by the moderate-polar and polar characters as well as higher surface area of these two resins, which led to stronger affinities with syringopicroside, an iridoid glycoside with moderate polarity. Although moderate-polar ADS-17 resin seems prone to enrich the polar target compound syringopicroside, its adsorption and desorption capacities were relatively lower due to too low surface area. ADS-8 is a nonpolar resin which also showed low adsorption capacity to the polar compound. Comparatively, weak-polar D141 resin with the greatest q_e and q_d values exhibited best adsorption and desorption behaviors for tested sample, probably because its specific surface area and average pore diameter are suitable for adsorbing and desorbing of syringopicroside. This behavior is expected, since the adsorption of syringopicroside molecules should occur in an aqueous environment mainly due to the van der Waals hydrophobic forces, which were stronger in the case of the weakly polar and moderate-polar resins. Thus, D141 resin was selected for further investigations of its separation behavior towards syringopicroside.

3.2. Adsorption Kinetics on D141 Resin. Adsorption kinetics curve for syringopicroside was obtained on D141. As shown in Figure 3, the adsorption capacity of D141 resin increased with the extension of adsorption time, and reaching equilibrium at about 3.5 h. In the initial 3 h, the adsorption capacity increased rapidly; after 3 h, the slope reached equilibrium which indicated the adsorption ratio varied little. Therefore, the duration of adsorption was set to 3 h in the following study.

3.3. Adsorption Isotherms on D14 Resin. The relationship between the concentration of solute and liquid phase at equilibrium is described by adsorption isotherms. Langmuir and Freundlich equations are used to reveal the linearity fitting and to describe how solutes interact with the resins. Langmuir equation assumes monomolecular layer adsorption with a homogeneous distribution of adsorption energies and without mutual interaction between adsorbed molecules [26]. The model of Langmuir can be expressed by the following mathematical formula:

$$q_e = \frac{q_m K C_e}{1 + K C_e}, \tag{4}$$

where q_e (mg/g) is the concentration of solute per mass of adsorbent (solid phase), also known as adsorptive capacity; C_e (mg/mL) is the concentration of solute in solution (liquid phase) at equilibrium; K (mg/g) is the Langmuir constant; q_m is the empirical constant. The Langmuir (4) was converted to the linearized form with C_e and C_e/q_e as independent variable, the experimental data were statistically analyzed and R^2 was obtained

$$\frac{C_e}{q_e} = \frac{C_e}{q_m} + \frac{1}{K} q_m. \tag{5}$$

The Freundlich model is an empirical equation, extensively used in the physical and chemical adsorption for nonideal adsorption systems, and it can be used to describe the adsorption behavior of monomolecular layer as well as that of the multimolecular layer. It assumes a heterogeneous distribution among the adsorption sites at different energies. It is a two-parameter model widely employed for many different adsorbate/adsorbent systems for liquid and gas phase adsorption [27]. The model of Freundlich can be expressed by the following mathematical formula:

$$q_e = K C_e^{1/n}. \tag{6}$$

Table 1: Physical properties of the test macroporous resins.

Name	Polarity	Particle diameter (mm)	Surface area (m^2/g)	Average pore diameter (nm)	Moisture content (%)
HPD450	Moderate polar	0.3~1.25	500~550	90~110	69.25
HPD600	Polar	0.3~1.25	500~550	75~110	67.73
ADS-17	Moderate polar	0.3~1.25	90~150	250~300	54.38
ADS-8	Nonpolar	0.3~1.25	450~500	120~160	56.82
D141	Weak polar	0.315~0.9	500~600	80~110	70.21
NKA-9	polar	0.3~1.25	250~290	155~165	48.47

A linearized form of Freundlich (6) can be written as

$$\ln q_e = \ln K + \frac{1}{n} \ln C_e, \quad (7)$$

where K is the Freundlich constant that is an indicator of adsorption capacity, and $1/n$ is an empirical constant related to the magnitude of the adsorption driving force. The K and n values can be obtained from the intercept and slope, respectively, and the linear regression line from a plot of $\ln q_e$ versus $\ln C_e$.

Equilibrium adsorption isotherms were constructed at the temperature of 25°C, 30°C, and 35°C. The initial concentrations of syringopicroside were 1.64, 2.05, 2.74, 3.28, 4.10, 4.92, 6.56, 8.20, and 11.48 mg/mL, respectively. As shown in Figure 4, the adsorption capacity of syringopicroside increased with the initial concentration and reached the saturation plateau when the initial concentration of syringopicroside was 6.56 mg/mL.

The Langmuir and Freundlich parameters were summarized in Table 2, where the correlation coefficients of Langmuir and Freundlich model were relatively high, and specifically the correlation coefficients of Langmuir equations of syringopicroside at different temperatures were all rather higher ($R^2 > 0.95$), indicating the adsorption process was mainly a monomolecular layer adsorption. It could describe the better adsorption behavior of this kind of iridoid glycoside on D141 resin.

Generally, in the Freundlich (6), the adsorption can take place easily when the $1/n$ value is between 0.1 and 0.5, and it is not easy to happen if $1/n$ value is between 0.5 and 1. Furthermore, the adsorption is very difficult to occur if $1/n$ value exceeds 1 [28]. In Table 2, the $1/n$ values are unambiguously between 0.1 and 0.5 which indicate that the adsorption of syringopicroside on D141 resin can take place easily and the resin is appropriate for the separation of this kind of iridoid glycoside. The result showed that both hydrophobic interaction and hydrogen bonding might exist between the D141 resin and syringopicroside molecule.

We can also see from Figure 4, within the range of temperatures investigated, at the same initial concentration, the adsorption capacities decreased with the increasing temperature; and the adsorption speed was slower than desorption speed, suggesting that the adsorption of syringopicroside on D141 resin resulted in the reduction of surface Gibbs' free energy of integral system, and the adsorption process was a thermopositive process. In addition, the dissolubility increased with the rising temperature, which could lead to lower adsorption capacity of the adsorbate. The lower adsorption temperature and higher desorption temperature are proper in industrial production. Therefore, 25°C was selected in the following experiments.

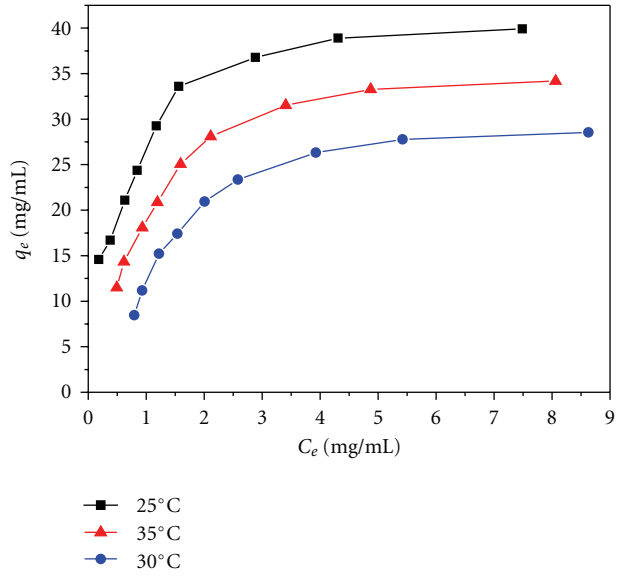

Figure 4: Adsorption isotherm curve of syringopicroside on D141 resin at 25, 30, and 35°C ($n = 3$).

3.4. Foundation of Chromatographic Method

3.4.1. Effect of the pH Value of Initial Solution on the Capacity of Adsorption. The pH value of sample solution is very important for the adsorption and desorption properties of resins, since the pH value determines the extent of ionization of solutes molecules, thereby affecting their adsorption affinity. Syringopicroside is a weakly acidic compound owing to the existence of a phenolic hydroxyl group. The adsorption property of the selected resin was therefore investigated at different pH values of adsorption solution. Preweighed hydrated adsorbent (equal to 3 g dry resin) was put into an Erlenmeyer flask containing 30 mL of aqueous solution of the crude extracts. The concentration of syringopicroside in sample solution was 6.56 mg/mL, and the flask was shaken (100 rpm) at 25°C. The concentration of syringopicroside in liquid phase was monitored by HPLC at the time of adsorption equilibration.

Table 2: Langmuir and Freundlich parameters of syringopicroside on D141 resin at different temperature.

Temperature (°C)	Langmuir equation	R^2	Freundlich equation	R^2
25	$C_e/q_e = 0.023C_e + 0.0129$	0.965	$q_e = 25.127C_e^{0.3041}$	0.932
30	$C_e/q_e = 0.0247C_e + 0.0268$	0.986	$q_e = 18.181C_e^{0.3920}$	0.901
35	$C_e/q_e = 0.0273C_e + 0.0485$	0.953	$q_e = 12.596C_e^{0.4819}$	0.847

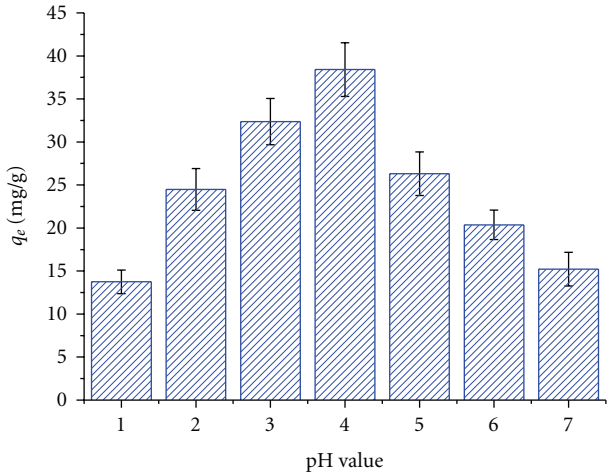

Figure 5: Effect of pH value on the adsorption capacity of syringopicroside on D141 resin ($n = 3$). Data are expressed as the mean ± standard deviation (Mean ± SD).

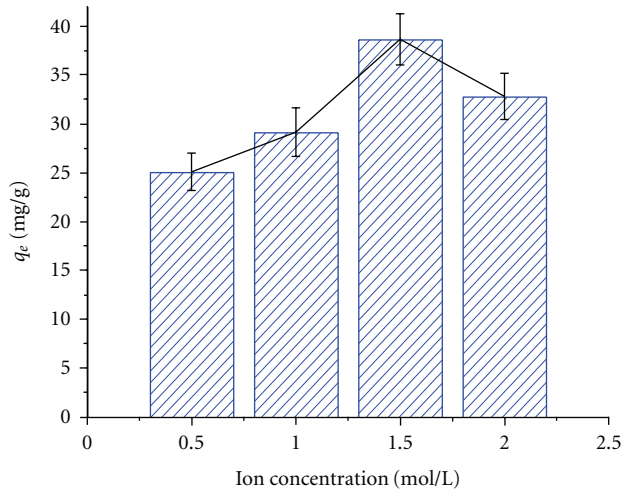

Figure 6: Effect of ion strength on the adsorption of syringopicroside ($n = 3$). Data are expressed as the mean ± standard deviation (Mean ± SD).

As shown in Figure 5, the highest adsorption capacity appeared at pH 4 value. The adsorption ratio of syringopicroside increased distinctly within pH values from 1 to 4. However, we observed a turning point at pH values higher than 4, the adsorption ratio of syringopicroside on D141 resin decreased obviously. In view of the structure of syringopicroside, the pH value influences the extent of ionization of syringopicroside, thus affecting the affinity between the solutes and solutions. At lower pH values, the surface of the resin would be surrounded by the hydronium ions which enhance the interaction of the unionized phenolic hydroxyl group of syringopicroside with the macroporous resin by greater attractive forces [29]. At higher pH values, the adsorption quantity of syringopicroside on D141 resin decreased linearly, which was probably caused by the reduced hydrogen-bonding interactions because the phenolic hydroxyl groups in syringopicroside dissociate to form H^+ and their corresponding anions, resulting in the decrease of adsorption capacity and adsorption ratio.

In addition, too lower pH value was inclined to cause hydrolysis of glycosides, leading to a decrease of syringopicrosides. Therefore, the pH value of the solution was adjusted to 4 for all later experiments.

3.4.2. Effect of the Ion Concentration of Initial Solution on the Capacity of Adsorption. The ion concentration influences the dissolubility of solutes, thus affecting the affinity between the solutes and solutions. The existence of salt ions led to a decrease of free water in solution and produced salting out effect which caused a degradation of the dissolubility of solutes. Therefore, the adsorption ratio of the solutes on the resin was enhanced. As shown in Figure 6, the adsorption quantity of syringopicrosides reached the highest point when the ion concentration of NaCl was 1.5 mol/L. It is thus evident that a certain extent of ion concentration increased the adsorption quantity of syringopicrosides, probably caused by the migration of adsorption equilibrium to adsorption direction due to salting out effect.

3.4.3. Dynamic Leakage Curve on D141 Resin. The dynamic leakage curve on D141 resin was obtained on the volume of effluent liquid and the concentration of syringopicroside herein. The results were shown in Figure 7.

Breakthrough volume is important in solid phase extraction because it represents the sample volume that can be preconcentrated without loss of analytes during the loading of sample. When the adsorption reaches the break point, the adsorption affinity decreases, even disappears, and the solutes leak from the resin. Therefore, it is important to set up the leakage curve in order to calculate the quantity of resin, the processing volume of sample solution, and the proper feeding flow rate of sample solution. The breakthrough point can be defined as 1–5% of the ratio of the exit solute concentration to the inlet solute concentration [30].

The initial concentration of syringopicroside in this test was 6.56 mg/mL, and the flow rate was set at 1, 2, and 4 BV/h, respectively. As shown in Figure 7, at the 5% breakpoint,

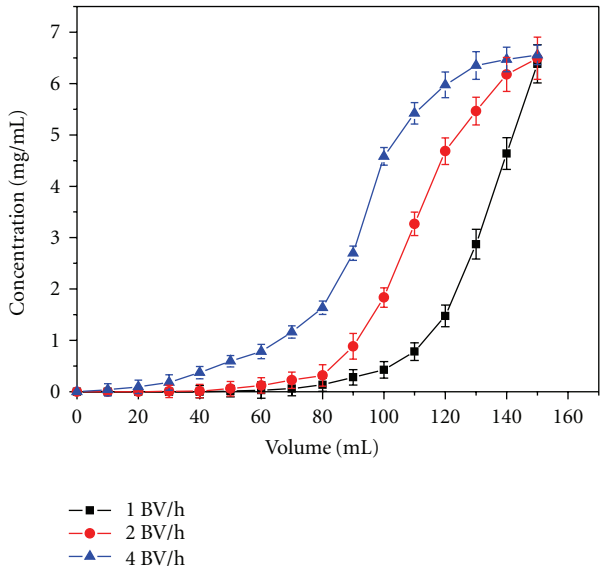

Figure 7: Dynamic leakage curves of syringopicroside from *F. syringae* leaves extract solution on D141 resin ($n = 3$). Data are expressed as the mean ± standard deviation (Mean ± SD).

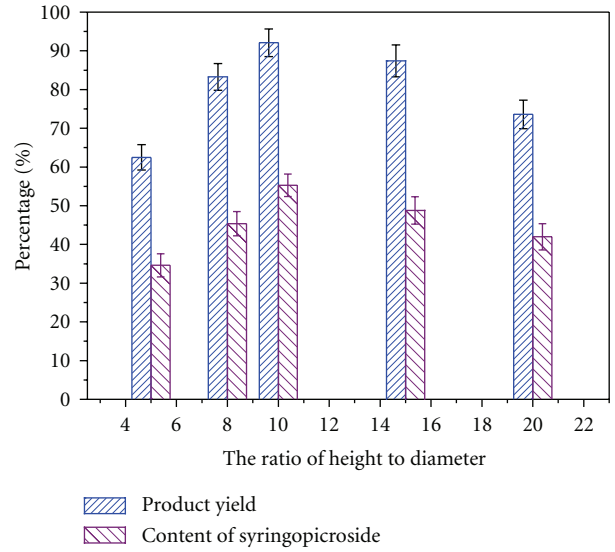

Figure 8: The effect of ratio of column height to diameter on syringopicroside yield and content ($n = 3$). Data are expressed as the mean ± standard deviation (Mean ± SD).

breakthrough volume of syringopicroside on D141 resin was 3.2, 2.8, and 1.7 BV corresponding to calculated adsorption capacities as 37.11, 36.52, and 26.27 mg/g resin. Because breakthrough adsorption capacities varied little at the flow rates of 1 and 2 BV/h, and too lower flow rate prolonged process time, thus 2 BV/h was selected as the suitable adsorption flow rate in further experiments. Under this condition, the processing volume of syringopicroside in sample solution on D141 resin was approximately 2.8 BV (83.5 mL), the total adsorption quantity was 547.76 mg, and the dynamic saturated adsorption quantity was 36.52 mg per gram resin.

3.4.4. Effect of the Ratio of Column Height to Diameter. The ratio of column height to diameter is very important for the adsorption and desorption properties of resins, since the ratio of column height to diameter determines the extent of saturated adsorption of syringopicroside molecules, thereby affecting their adsorption affinity. Lower ratio implied low mass transfer rate due to a short interaction time between syringopicroside molecule and adsorbent, and the adsorbate will leak out easily. While too higher ratio indicated insufficient use of the bed, as well as the insufficient desorption leading to lower recovery of the products. As shown in Figure 8, the ratio 10 was ideal among the 5 trials.

3.4.5. Effect of Concentration of Ethanol Solution on the Ratio of Desorption. Different concentrations of ethanol solutions were used to perform desorption tests in order to choose proper desorption solution. As shown in Figure 9, with the increasing of ethanol concentration, the desorption ratio of syringopicroside increased accordingly and reached the peak value at concentration of (70 : 30, v/v) ethanol-water solution, in which the desorption ratio and the content

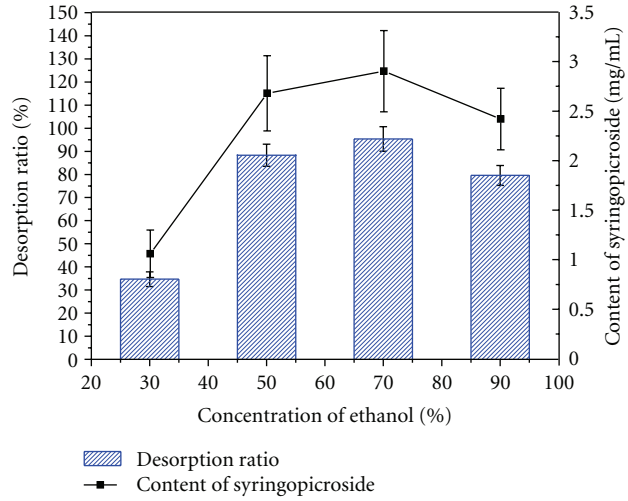

Figure 9: Effect of concentration of ethanol solution on the desorption ratio and content of syringopicroside ($n = 3$). Data are expressed as the mean ± standard deviation (Mean ± SD).

of syringopicroside were 95.38% and 2.903 mg/mL, respectively. However, the desorption ratio and the content of syringopicroside decreased when the ethanol concentration reached 90%. Therefore, ethanol-water (70 : 30, v/v) solution was selected as the appropriate desorption solution and was used in the following tests.

3.4.6. Dynamic Desorption Curve on D141 Resin. It is important to choose a proper flow rate to desorb syringopicroside from the resin effectively. The ethanol-water solution (70 : 30, v/v) was used to elute syringopicroside with its flow rate set at 1, 2, 3, 4, and 5 BV/h. As can be seen in Figure 10, syringopicroside was totally desorbed in 5 BV at the flow rate 1 BV/h; however, the elution process consumes too long time.

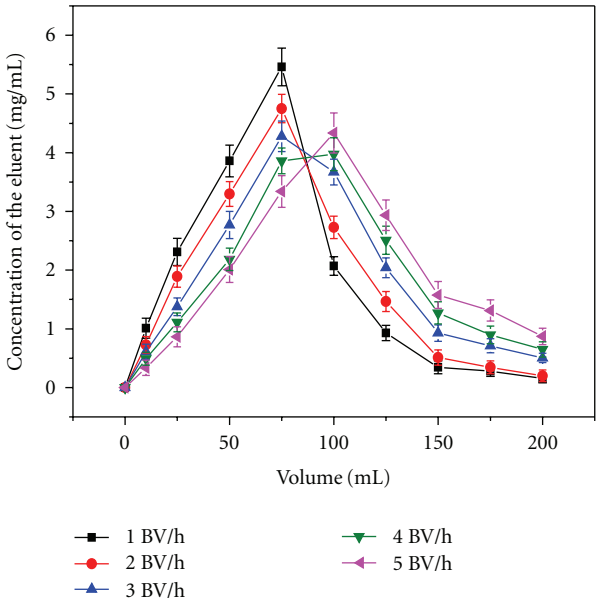

Figure 10: Dynamic desorption curve on D141 resin ($n = 3$). Data are expressed as the mean ± standard deviation (Mean ± SD).

Table 3: Enrichment and recovery results obtained for syringopicroside separated on column packed with D141 resin ($n = 3$).

Compound	Initial content in crude extracts (%)	Content in final product (%)	Recovery yield (%)	RSD for recovery yield (%)
Syringopicroside	2.32	55.74	92.16	1.86

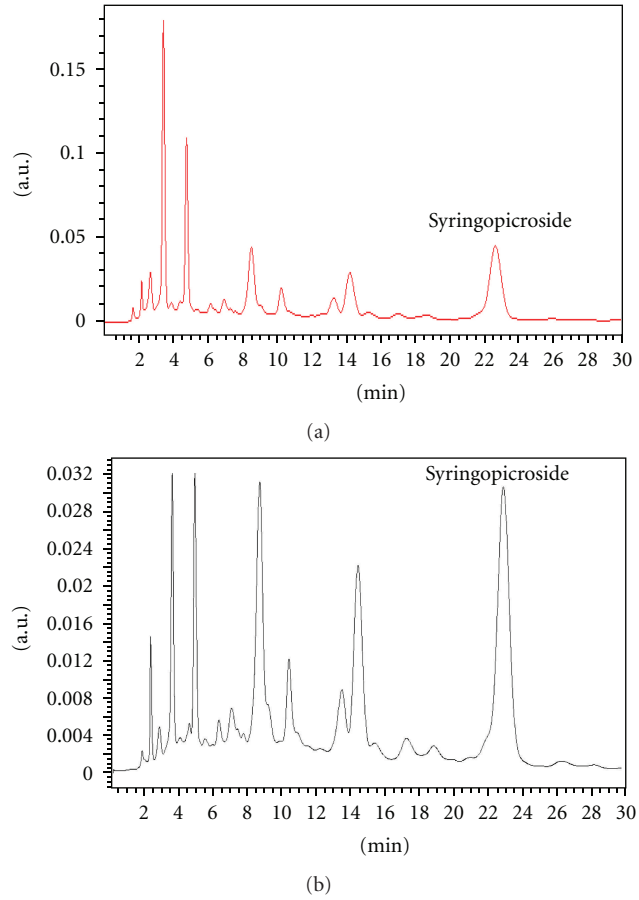

Figure 11: Chromatograms of sample solution before (a) and after (b) separation on column packed D141 resin.

The ideal desorption process was evident when the volume of eluent was approximately 180 mL (6 BV) at the flow rate 2 BV/h (Figure 10), in which better desorption performance of syringopicroside was exhibited due to better particle diffusion in sample solutions. With the flow rate rising, it consumed large volume of eluent, and syringopicroside was totally desorbed in 8, 9, and 10 BV (Figure 10). Therefore, the flow rate of 2 BV/h and the eluting volume of 6 BV were selected as the proper desorption flow rate and volume in consideration of the efficiency.

The desorption solution was analyzed by HPLC. The dynamic adsorption and desorption tests were repeated for three times under optimal conditions, and the RSD for recovery yield was calculated for syringopicroside. The results were shown in Table 3.

Table 3 showed that, after treatment with D141 resin, the content of syringopicroside reached 55.74%, which was 24-fold to that in *F. syringae* leaves crude extracts, and the recovery yield of syringopicroside was 92.16%. The chromatograms of the tested samples before and after treatment with D141 resin were shown in Figure 11. By comparison, it can be seen that some impurities were removed, and the relative peak area of syringopicroside increased obviously through separation on D141 resin. The results demonstrated a good selectivity of the adsorption and desorption process for recovering syringopicroside from the sample solution of *F. syringae* leaves extracts.

Therefore, the optimum parameters for the enrichment and preparative separation of syringopicroside with D141 macroporous resin were confirmed as following conditions. The ratio of column height to diameter is 10; for adsorption process, the concentration of syringopicroside in sample solution was 6.56 mg/mL, the ion concentration of NaCl was 1.5 mol/L, processing volume was 2.8 BV, pH 4, and temperature was 25°C; in desorption process, impurity was detached with 4 BV deionized water firstly, then syringopicroside was desorbed by 6 BV ethanol-water solution (70 : 30, v/v) with its flow rate at 2 BV/h.

4. Conclusions

In this study, a novel method of adsorption and separation with macroporous resin was developed offering feasible and reliable recovery of syringopicroside from the remainder extracts of *F. syringae* leaves. The adsorption and desorption properties of six macroporous resins were investigated by static adsorption and desorption test, and the separation process of the extracts from *F. syringae* leaves with selected resin was investigated by dynamic adsorption and desorption experiments. Among the six resins investigated, D141 resin

provided the highest separation power for syringopicroside. Process parameters including concentration and pH value of sample solution, solution volume, temperature, and so forth were optimized for the most effective separation of syringopicroside by D141 resin. The equilibrium experimental data of the adsorption of syringopicroside on D141 resin at 25°C fitted well to Langmuir and Freundlich isotherms, describing the adsorbate/adsorbent behavior within the concentration range studied. The optimized adsorption and desorption conditions were as follows: processing volume was 2.8 BV; concentration of syringopicroside in feeding solution was 6.56 mg/mL, ion concentration was 1.5 mol/L, pH value was 4, flow rate was 2 BV/h, and temperature was 25°C. The elution conditions were as follows: deionized water 4 BV, followed by 6 BV ethanol-water solution (70 : 30, v/v) with its flow rate 2 BV/h. Under these optimal conditions, the content of syringopicroside in the final product was 24-fold of that in *F. syringae* leaves crude extracts, and the recovery of syringopicroside was 92.16%. In conclusion, this adsorption-desorption study provided an effective and practical method with high yields and reliable recovery for enrichment and purification of syringopicroside from extracts of *F. syringae* leaves than conventional methods, because of its lower cost, nontoxic, high efficiency, and procedural simplicity.

Acknowledgment

The authors gratefully acknowledge the financial support by the Specialized Research Fund for the Doctoral Program of Higher Education of China (SRFDP) (Program no. 20060228005).

References

[1] P. A. Solomon and C. Sioutas, "Continuous and semicontinuous monitoring techniques for particulate matter mass and chemical components: a synthesis of findings from EPA's particulate matter supersites program and related studies," *Journal of the Air and Waste Management Association*, vol. 58, no. 2, pp. 164–195, 2008.

[2] Editorial Board of China Heral, State Administration of Traditional Chinese Medicine, *China Herbal*, Shanghai Scientific and Technical Publishers, Shanghai, China, 1999.

[3] Drug standard of Ministry of Public Health of China, Page number: Capsule Z20-176, Tablet Z9-10; Standard number: Capsule WS3-B-3881-98, Tablet WS3-B-1760-94.

[4] H. Oh, E. K. Ko, D. H. Kim et al., "Secoiridoid glucosides with free radical scavenging activity from the leaves of Syringa dilatata," *Phytotherapy Research*, vol. 17, no. 4, pp. 417–419, 2003.

[5] J. Xue, N. Zhang, and H. Teng, "The antiviral effect of the Chinese Medicine JiaDing Capsule," *Journal of Information on Traditional Chinese Medicine*, vol. 14, no. 2, pp. 47–48, 1997.

[6] Q. Chen, *Pharmacodynamic Action and Clinical Research of Chinese Patent Medicine Classical Prescription*, The People Health, Beijing, China, 1st edition, 1998.

[7] V. Kostyuk, A. Potapovich, T. Suhan et al., "Plant polyphenols against UV-C-induced cellular death," *Planta Medica*, vol. 74, no. 5, pp. 509–514, 2008.

[8] Y. Luo, Y. Liu, H. Qi, Z. Wu, and G. Zhang, "Steryl esters and phenylethanol esters from *Syringa komarowii*," *Steroids*, vol. 71, no. 8, pp. 700–705, 2006.

[9] K. MacHida, N. Ohkawa, A. Ohsawa, and M. Kikuchi, "Two new phenolic glycosides from Syringa reticulata," *Journal of Natural Medicines*, vol. 63, no. 2, pp. 192–194, 2009.

[10] Y. Takenaka, N. Okazaki, T. Tanahashi, N. Nagakura, and T. Nishi, "Secoiridoid and iridoid glucosides from Syringa afghanica," *Phytochemistry*, vol. 59, no. 7, pp. 779–787, 2002.

[11] L. Zhou, X. Feng, K. Huang, L. He, X. Deng, and D. Wang, "Studies on chemical constituents of *Syringa veutina*," *Journal of Chinese Medicinal Materials*, vol. 31, no. 5, pp. 679–681, 2008.

[12] D. L, P. Li, and J. Li, "Studies on active components of Syringa oblata Lindl leaves," *Chinese Traditional and Herbal Drugs*, vol. 34, no. 8, pp. 688–689, 2003.

[13] K. Machida, E. Unagami, H. Ojima, and M. Kikuchi, "Studies on the constituents of *Syringa* species. XII. New glycosides from the leaves of Syringa reticulata (BLUME) HARA," *Chemical and Pharmaceutical Bulletin*, vol. 51, no. 7, pp. 883–884, 2003.

[14] K. Machida, A. Kaneko, T. Hosogai, R. Kakuda, Y. Yaoita, and M. Kikuchi, "Studies on the constituents of Syringa Species. X. Five new iridoid glycosides from the leaves of Syringa reticulata (Blume) Hara," *Chemical and Pharmaceutical Bulletin*, vol. 50, no. 4, pp. 493–497, 2002.

[15] H. Li, J. H. Lee, and J. M. Ha, "Effective purification of ginsenosides from cultured wild ginseng roots, red ginseng, and white ginseng with macroporous resins," *Journal of Microbiology and Biotechnology*, vol. 18, no. 11, pp. 1789–1791, 2008.

[16] Y. Fu, Y. Zu, W. Liu et al., "Optimization of luteolin separation from pigeonpea [Cajanus cajan L. Mill sp.] leaves by macroporous resins," *Journal of Chromatography A*, vol. 1137, no. 2, pp. 145–152, 2006.

[17] E. M. Silva, D. R. Pompeu, Y. Larondelle, and H. Rogez, "Optimisation of the adsorption of polyphenols from Inga edulis leaves on macroporous resins using an experimental design methodology," *Separation and Purification Technology*, vol. 53, no. 3, pp. 274–280, 2007.

[18] B. Fu, J. Liu, H. Li, L. Li, F. S. C. Lee, and X. Wang, "The application of macroporous resins in the separation of licorice flavonoids and glycyrrhizic acid," *Journal of Chromatography A*, vol. 1089, no. 1-2, pp. 18–24, 2005.

[19] Y. Fu, Y. Zu, W. Liu et al., "Preparative separation of vitexin and isovitexin from pigeonpea extracts with macroporous resins," *Journal of Chromatography A*, vol. 1139, no. 2, pp. 206–213, 2007.

[20] M. Huang, Y. Xu, Q. Lv, and Q. Ren, "Separation and purification off β-carotene from chlorophyll factory residues," *Chemical Engineering and Technology*, vol. 31, no. 6, pp. 922–927, 2008.

[21] C. Ma, G. Tao, J. Tang et al., "Preparative separation and purification of rosavin in *Rhodiola rosea* by macroporous adsorption resins," *Separation and Purification Technology*, vol. 69, no. 1, pp. 22–28, 2009.

[22] X. Liu, Y. J. Gao, J. M. Wang, G. J. Xu, and H. M. Xue, "Enrichment process of syringopicroside in Folium Syringae Oblatae with macroporous resin," *Chinese Traditional and Herbal Drugs*, vol. 39, no. 11, pp. 1655–1659, 2008.

[23] N. Nenadis, J. Vervoort, S. Boeren, and M. Z. Tsimidou, "*Syringa oblata Lindl var. alba* as a source of oleuropetn and related compounds," *Journal of the Science of Food and Agriculture*, vol. 87, no. 1, pp. 160–166, 2007.

[24] Y. Fu, Y. Zu, S. Li et al., "Separation of 7-xylosyl-10-deacetyl paclitaxel and 10-deacetylbaccatin III from the remainder extracts free of paclitaxel using macroporous resins," *Journal of Chromatography A*, vol. 1177, no. 1, pp. 77–86, 2008.

[25] D. S. Grzegorczyk and G. Carta, "Adsorption of amino acids on porous polymeric adsorbents—I. Equilibrium," *Chemical Engineering Science*, vol. 51, no. 5, pp. 807–817, 1996.

[26] I. Langmuir, "A new adsorption isotherm," *The Journal of the American Chemical Society*, vol. 40, no. 9, pp. 1361–1403, 1918.

[27] M. Scordino, A. Di Mauro, A. Passerini, and E. Maccarone, "Adsorption of flavonoids on resins: cyanidin 3-glucoside," *Journal of Agricultural and Food Chemistry*, vol. 52, no. 7, pp. 1965–1972, 2004.

[28] R. Traybal, *Mass Transfer Operation*, Mocraw-Hill, Singapore, 1981.

[29] B. Zhang, R. Yang, Y. Zhao, and C. Z. Liu, "Separation of chlorogenic acid from honeysuckle crude extracts by macroporous resins," *Journal of Chromatography B*, vol. 867, no. 2, pp. 253–258, 2008.

[30] M. W. Jung, K. H. Ahn, Y. Lee et al., "Evaluation on the adsorption capabilities of new chemically modified polymeric adsorbents with protoporphyrin IX," *Journal of Chromatography A*, vol. 917, no. 1-2, pp. 87–93, 2001.